Crystallization Behavior and Phase-Transformation Mechanism with the Use of Graphite Nanosheets in Poly(vinylidene fluoride) Nanocomposites

Y. Y. Zhang, S. L. Jiang, Y. Yu, Y. K. Zeng, G. Z. Zhang, Q. F. Zhang., J. G. He

Department of Electronic Science and Technology, Huazhong University of Science and Technology, Wuhan, 430074, People's Republic of China

Received 4 May 2011; accepted 2 September 2011
DOI 10.1002/app.35627
Published online 16 January 2012 in Wiley Online Library (wileyonlinelibrary.com).

ABSTRACT: Poly(vinylidene fluoride) (PVDF)–graphite nanosheet (GNS) nanocomposites with different contents of GNSs were prepared by the solution-casting method. The GNSs were produced by the ultrasonic exfoliation of graphite. The effects of GNSs on the crystalline structure, degree of the crystallization, conductivity, and phase-transformation mechanism of PVDF were investigated. Atomic force microscopy data showed that the GNSs had a flake-shaped nanostructure. Fourier transform infrared spectroscopy and X-ray diffraction results revealed that a β phase formed with the addition of GNSs, and the phase-transformation mechanism from the α phase to the β phase of PVDF was confirmed. Differential scanning calorimetry results indicated that addition of GNSs led to an increased melting temperature and increased degree of crystallization; this implied that the GNSs acted as nucleating agents. © 2012 Wiley Periodicals, Inc. J Appl Polym Sci 125: E314–E319, 2012

Key words: films; nanocomposites; nucleation

INTRODUCTION

Polymer nanocomposites have gained extensive attention in the past decade because of the improvement in their physical properties and electrical properties compared with original polymer matrices.[1–4] Poly (vinylidene fluoride) (PVDF) as a polymer matrix is a particularly interesting and attractive polymer material because of its flexible and outstanding piezoelectric properties.[5,6] PVDF is a semicrystalline polymer. It exhibits five crystalline phases[7] known as the nonpolar TGTG′ α phase, δ phase, polar TTTT β phase, and TTTGTTTG′ γ and ε phases, where T and G are the trans and gauche chain conformations found in the PVDF crystal. When PVDF is cooled from the melt, the crystalline phase formed is a nonpolar phase.[8] The β-phase crystal has an all-trans conformation that results in the most polar phase among other crystals and is used extensively in piezoelectric, pyroelectric, and ferroelectric applications.[9,10]

Unfortunately, the α phase is thermodynamically more stable in PVDF than the β phase. There have been numerous attempts to stabilize this phase. The β phase of PVDF can be obtained by crystallization from certain solutions,[11] crystallization from solution under special conditions,[12,13] induction by substrate,[14] the incorporation of halide,[15,16] carbon tubes,[17,18] or carbon fibers.[19,20] One effective way to obtain β-phase PVDF is through mechanical stretching,[21,22] but it is not suitable for film samples on a substrate. There have also been some studies on the addition of clay.[23–25] Shah et al.[26] and Yu et al.[27] observed that the addition of clay led to the β phase of PVDF. They assumed that a possible mechanism for the stabilization of the β phase was that the nanoclay provided the substrates of PVDF nucleation. Similar to the clay, natural flake graphite is another layered material. The graphite crystal lattice consists of graphene layers formed by sp^2 hybridization, whereas the carbon sheets are bound by weak van der Waals interactions.[28,29] Graphite nanosheets (GNSs), consisting of superimposed lamellae of two-dimensional carbon–carbon covalent networks, have a large area and nanothickness, a high mechanical strength, superior transport properties, and giant thermoelectric properties, which may lead to the formation of high-performance nanocomposites.

In this work, we report on an investigation of the dispersion and exfoliation of natural graphite to prepare two-dimensional GNSs. PVDF/GNS nanocomposites with different GNS volumes from 1 to 7 mL were prepared as films via a solution-casting method.

Correspondence to: S. L. Jiang (jslhust@gmail.com).
Contract grant sponsor: Innovation Research Fund of Huazhong University of Science and Technology; Colleges and universities in Hubei province the provincial teaching research project (2011065); National Nature Science Foundation of China (51102102); National Defense Key Laboratory of Ministry of Education (0196185003); National High Technology Research and Development Program of China; contract grant number: 2007AA03Z120.

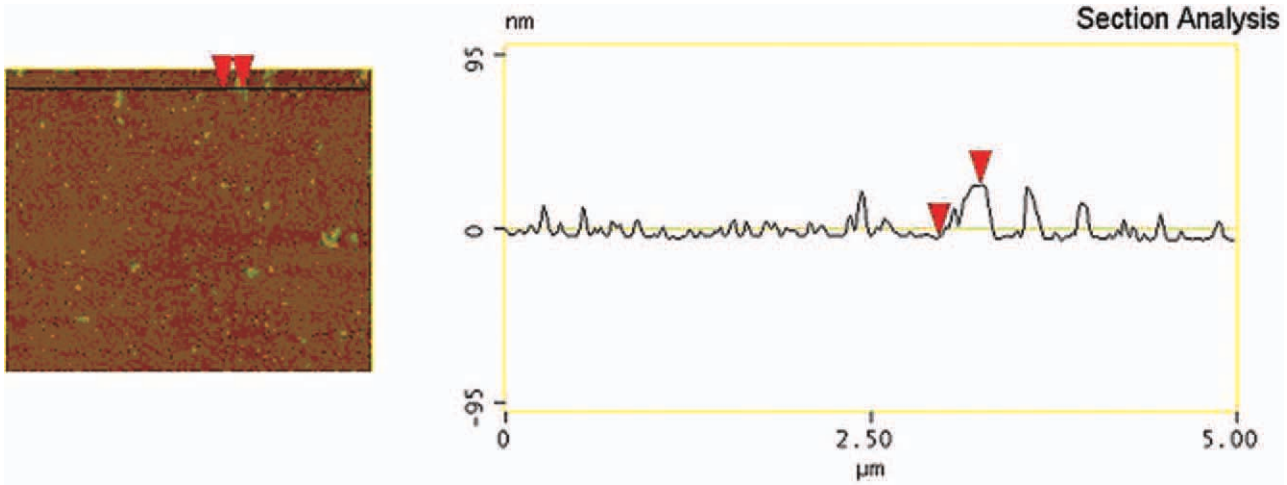

Figure 1 Noncontact mode AFM image of the GNSs with height profiles. [Color figure can be viewed in the online issue, which is available at wileyonlinelibrary.com.]

With the presence of different amount of GNSs, we investigated the crystalline structure and degree of crystallization of the PVDF/GNS nanocomposites. The formation mechanism of the β phase is proposed.

EXPERIMENTAL

Raw materials

The PVDF powder used in this study was a product of Academic of Sichuan Chenguang Chemical Center (Sichuan, China). The N,N-dimethylformamide (DMF) solvent and graphite powder were both bought from Senopharm Chemical Reagent Co., Ltd. (Shanghai, China).

Sample preparation

The GNSs were prepared by exfoliation from graphite as the reference.[30] In the experiment, 0.02 g of graphite was dispersed in 40 mL of DMF solvent by high-shear mixing for 1 h; this was followed by bath sonication for 6 h (sonic power = 320 W) to obtain GNS dispersions. To remove large aggregates, the dispersion was mildly centrifuged at 300 rpm for 90 min, and 30 mL of supernatant was retained.

PVDF (216 mg) was dissolved in DMF and mixed with different volumes of GNS supernatant in 15 mL of DMF. The PVDF/GNS mixture solution was mechanically stirred at room temperature for 1 h and then sonicated for 1 h before it was poured into uncovered glass dishes, which were heated at 100°C for 1 day to ensure the removal of the solvent traces. The films had thicknesses in the range 0.08–0.09 mm. The loading levels of the nanocomposite films were 0, 1, 2, 3, 4, 5, 6, and 7 mL of GNS supernatant.

Tapping-mode atomic force microscopy (AFM) images of the GNSs were obtained on the silicon substrate with a NanoFirst-3000 tapping-mode atomic force microscope(Veeco, America). The crystalline structure analysis was performed at room temperature by Fourier transform infrared (FTIR) spectroscopy (VERTEX 70, Bruker, Germany) in the range 550–1500 cm^{-1}. X-ray diffraction (XRD) experiments were performed at room temperature with Cu Kα radiation with a PANalytical B. V. XRD instrument. The wavelength of the X-ray was 0.154059 nm. All XRD data were collected from $2\theta = 10–26°$ with a step interval of 0.02°. We collected the data by scanning the top surface of the corresponding films. Differential scanning calorimetry (DSC) analysis was performed with a WCR-2C DSC instrument(Beijing, China) in a nitrogen atmosphere. The specimens were heated at a rate of 5°C/min from 115 to 197°C. The specimens were weighed accurately at 19 mg.

RESULTS AND DISCUSSION

To characterize the shape parameter of the species, the GNS solutions were spin-coated and evaporated on silicon. AFM measurements in tapping mode were used to investigate the thickness and shape of the GNSs (Fig. 1). It could be seen that the graphite sheets had a flake structure and varied shapes and sizes, with a measured thickness of 25 nm.

The FTIR spectra of the PVDF/GNS nanocomposites with different GNS volumes (0, 1, 5, 6, and 7 mL) were carried out to ascertain the presence of the β phase in the PVDF matrix, as shown in Figure 2. The bands at 615, 765, 795, 1182, and 1400 cm^{-1} referred to the TGTG′ conformer of the α phase, whereas the bands at 840, 1233, and 1270 cm^{-1} corresponded to when the chain had a longer trans sequence than TT. The bands were characteristic of β- or γ-phase crystals, which contain TTT or TTTGTTTG′, respectively.[31] The 765-cm^{-1} band corresponded to the vibration mode of the in-plane

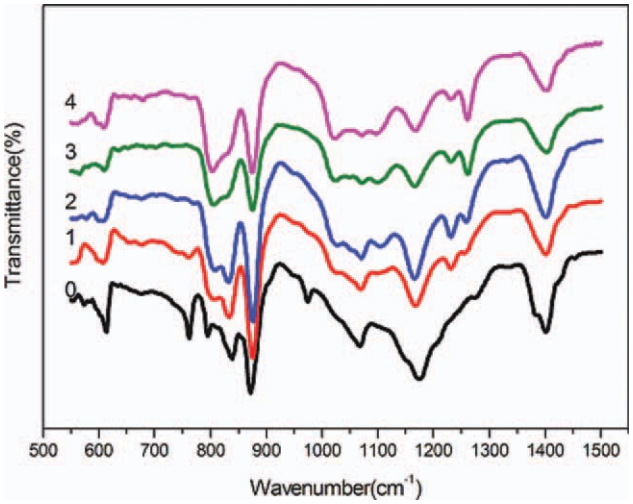

Figure 2 FTIR spectra of the PVDF/GNS nanocomposites (0) PVDF–GNS (0 mL), (1) PVDF–GNS (1 mL), (2) PVDF–GNS (5 mL), (3) PVDF–GNS (6 mL), and (4) PVDF–GNS (7 mL). [Color figure can be viewed in the online issue, which is available at wileyonlinelibrary.com.]

bending or rocking of CH_2 of the PVDF α phase. We should note that the band at 840 cm^{-1} was related to a mixed mode of CH_2 rocking and CF_2 asymmetric stretching vibrations of the PVDF β phase. From the figure, it is apparent that pure PVDF had peaks at 615, 765, 795, 1182, and 1400 cm^{-1}. With increasing GNS content, the bands at 765 and 795 cm^{-1}, belonging to the α phase, vanished, and the bands at 840 and 1270 cm^{-1}, which referred to the β phase, increased relatively, whereas the band at 1233 cm^{-1}, belonging to the γ phase, also increased relatively. Our FTIR results suggested that the GNSs could have induced the β and γ phases and reduced the α phase in the PVDF/GNS nanocomposites.

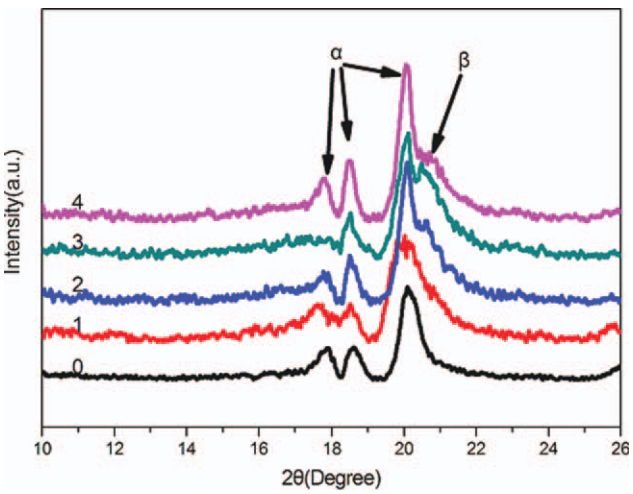

Figure 3 XRD analysis of the PVDF/GNS nanocomposites: (0) PVDF–GNS (0 mL), (1) PVDF–GNS (1 mL), (2) PVDF–GNS (5 mL), (3) PVDF–GNS (6 mL), and (4) PVDF–GNS (7 mL). [Color figure can be viewed in the online issue, which is available at wileyonlinelibrary.com.]

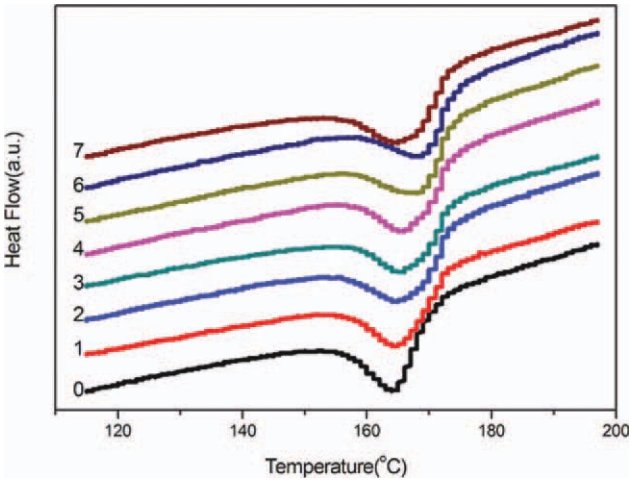

Figure 4 DSC scans of the PVDF/GNS nanocomposites: (0) PVDF–GNS (0 mL), (1) PVDF–GNS (1 mL), (2) PVDF–GNS (2 mL), (3) PVDF–GNS (3 mL), (4) PVDF–GNS (4 mL), (5) PVDF–GNS (5 mL), (6) PVDF–GNS (6 mL), and (7) PVDF–GNS (7 mL). [Color figure can be viewed in the online issue, which is available at wileyonlinelibrary.com.]

The results of XRD analysis of the PVDF and PVDF/GNS nanocomposites are shown in Figure 3. From the integration of the area under the crystalline peaks, it can be seen that the figure contains predominantly major crystalline peaks at 2θ values of 17.7, 18.4, 19.9, and 20.7°. These peaks at 17.7, 18.4, and 19.9° were attributed to the crystal planes associated with the α phase, and the peak at 20.7° was related to the β phase.[32] With the addition of GNSs, a change in the relative intensity of peaks could be clearly seen. The increasing in GNS contents gradually decreased the peak at 17.7° (α phase), and the peak finally vanished when 6 mL of GNSs was added and then reappeared with further addition. In contrast, the peak at 19.9° became a shoulder with the addition of GNSs. The peak at 20.7° appeared when 5 mL of GNSs was added, increased when 6 mL of GNSs was added, and then decreased with further addition. Our XRD results showed that the β phase increased with GNS addition, reached the maximum amount when 6 mL of GNSs was added, and decreased with further addition. This suggested that some agglomeration might have occurred in the GNSs, which decreased the chain confinement, even for decreased degrees of crystallization of the PVDF/GNS nanocomposites, which were confirmed by the DSC results.

DSC was performed in the PVDF/GNS nanocomposites, as shown in Figure 4; it could determine the degree of crystallization and the thermal properties of the samples, as shown in Figures 5 and 6. The incorporation of GNSs in the nanocomposites had a direct influence on the degree of crystallization and the thermal properties of PVDF.

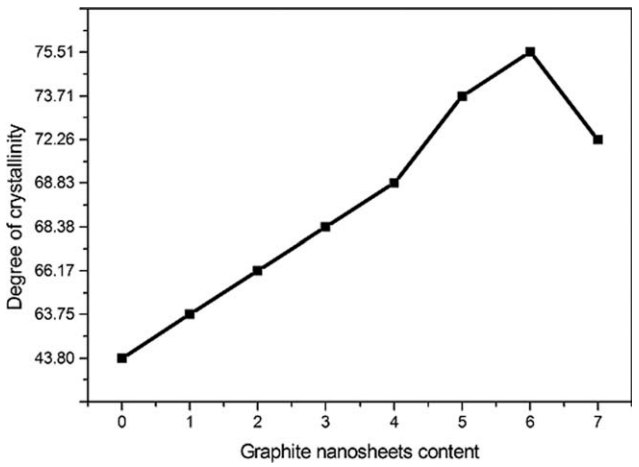

Figure 5 Degree of crystallization of the PVDF/GNS nanocomposites: (0) PVDF–GNS (0 mL), (1) PVDF–GNS (1 mL), (2) PVDF–GNS (2 mL), (3) PVDF–GNS (3 mL), (4) PVDF–GNS (4 mL), (5) PVDF–GNS (5 mL), (6) PVDF–GNS (6 mL), and (7) PVDF–GNS (7 mL).

The degree of crystallization (ΔX_c) of the PVDF films could be obtained as follows:

$$\Delta X_c = \frac{\Delta H_m}{\Delta H_{100\%,\text{crystalline}}} \quad (1)$$

where ΔH_m is the melting enthalpy of the samples and $\Delta H_{100\%,\text{crystalline}}$ is the melting enthalpy for a 100% crystallized sample of pure PVDF, which was reported to be 104.6 J/g.[33]

Figure 5 shows the degree of crystallization of the PVDF films with the feeling content. Obviously, an increase in the degree of crystallization of the nanocomposites was observed compared to the pure samples of PVDF. This indicated that the GNSs acted as nucleation agents in the composites and promoted the degree of crystallization of the PVDF matrix. With increasing GNS concentration, the degree of crystallization increased gradually and reached the highest improvement for nanocomposites with 6 mL of GNSs. When more GNSs were added, the degree of crystallization decreased. This was because excessive GNSs confined the movements of polymer chains, which resulted in a decrease of the degree of crystallization. It could be inferred that 6 mL of GNSs was a critical nanofiller concentration in the PVDF/GNS nanocomposites.

In addition, it could be seen that the presence of GNSs had effects on the shift of the onset temperature of melting and the melting temperature of the PVDF/GNS nanocomposites. With increasing GNS content, the melting temperature of the composites increased earlier and then decreased with further additions. This could be attributed to more β phase contained in the composites with increasing GNSs; this was consistent with the results of XRD. When more GNSs were added, excessive GNSs confined the movements of the polymer chains and decreased the crystallization of PVDF; then, the onset temperature of melting and the melting temperature decreased.

An overall picture of GNS dispersion, interactions with PVDF, and β-phase formation are given Figure 7. The β phase consisted of TTTT conformation chains, whereas the α phase consisted of TGTG′ conformation chains. The GNSs consisted of graphene layers formed by sp^2 hybridized carbon atoms, which had a large electronegativity (2.55). Furthermore, the fluorine in PVDF had extreme electronegativity (3.98), whereas the hydrogen had a small electronegativity. The C—F bond in PVDF carried a permanent strong electric moment of 7×10^{-30} cm.[34] The GNSs acted as nucleation agents in the PVDF matrix during the crystallization of the nanocomposites. The formation of numerous β phases was attributed to an interaction between the GNSs and PVDF molecular chains; this affected the motion and ordered arrangement of the polymer chains. During polymer crystallization, there existed dipolar intermolecular interactions between PVDF and DMF, and the GNSs acted as nucleation agents. Polar moieties of DMF tended to rotate the strong dipoles of C—F bonds around the C—C bonds of the chain backbone and made the PVDF chains wind on the GNS surface, as proposed by Salimi and Yousefi.[12] The F atoms were easily induced to arrange along the GNSs in the same orientation; this favored the formation of the all-trans conformation β-PVDF finally. The driving force of polymer intercalation from solution was the entropy gained by desorption of the

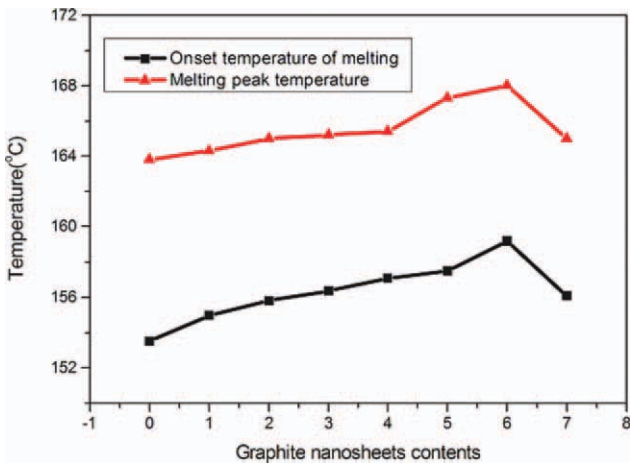

Figure 6 Thermal properties of the PVDF/GNS nanocomposites: (0) PVDF–GNS (0 mL), (1) PVDF–GNS (1 mL), (2) PVDF–GNS (2 mL), (3) PVDF–GNS (3 mL), (4) PVDF–GNS (4 mL), (5) PVDF–GNS (5 mL), (6) PVDF–GNS (6 mL), and (7) PVDF–GNS (7 mL). [Color figure can be viewed in the online issue, which is available at wileyonlinelibrary.com.]

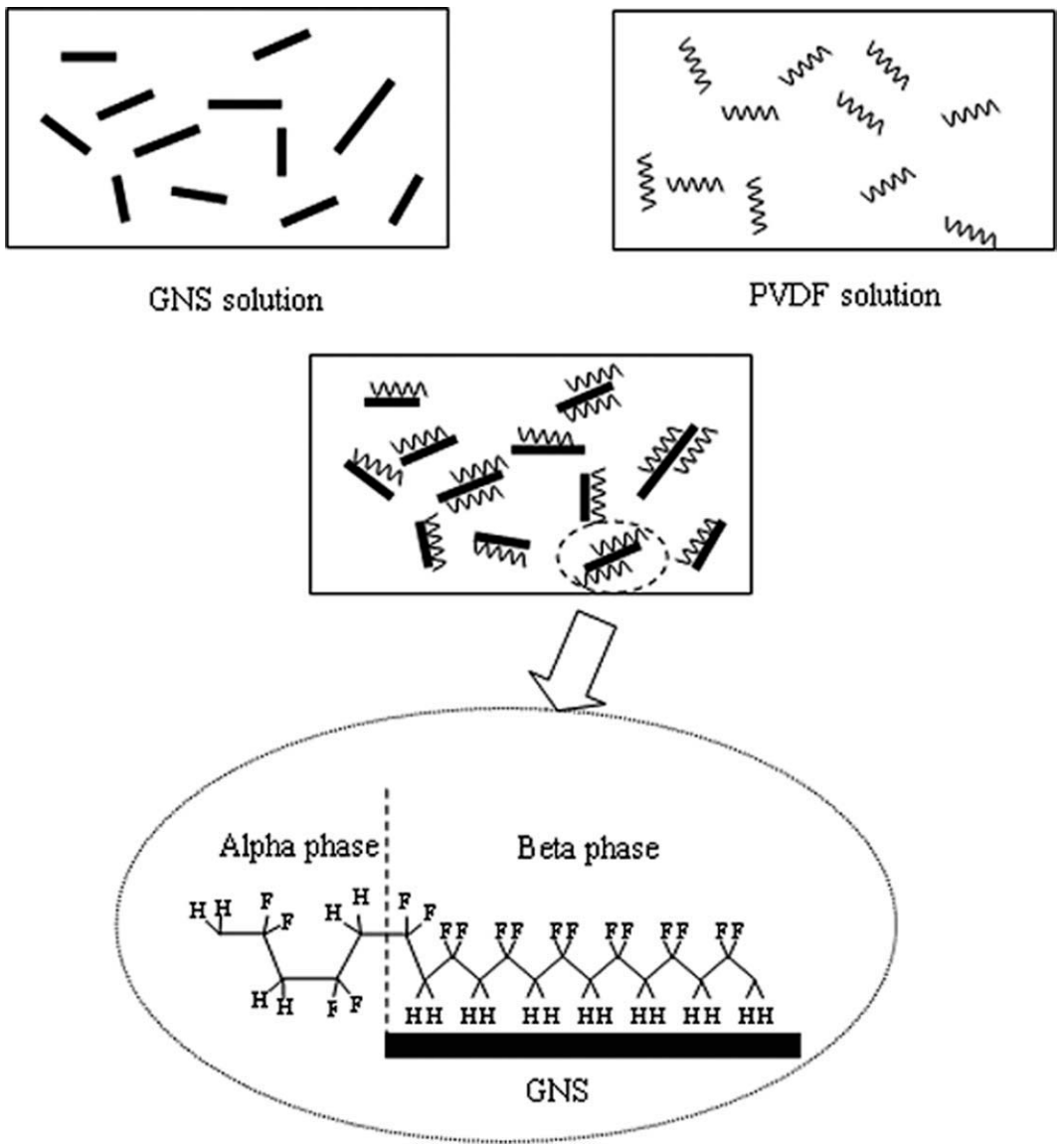

Figure 7 Schematic showing the proposed mechanism about β-phase formation.

solvent molecules; this compensated for the decrease in conformational entropy of the intercalated polymer chains.[35] In addition, this intercalation only existed on the surface of GNS. That is the reason why there still existed a certain amount of α phase in the nanocomposites. When the solvent was evaporated, the GNSs reassembled, sandwiching the polymer to form the nanocomposites.

CONCLUSIONS

GNSs were prepared by the exfoliation of natural graphite. PVDF nanocomposite films filled with different volumes of GNSs were prepared by the solution-casting method. The AFM results showed that the GNSs had a flake nanostructure, with a measured thickness of 25 nm. Both XRD and FTIR data indicated that the nanocomposites had the β-phase structure because of the addition of GNS, which stabilized the TTTT long chains. The DSC results indicated a shift in the melting temperature of the nanocomposites to a higher degree with increasing GNSs. An increase of the crystallization degree of the nanocomposite was observed compared with the pure PVDF samples. This indicated that the GNSs acted as nucleation agents in the nanocomposites and increased the degree of crystallization in the PVDF matrix. Because of a strong interaction between GNS and PVDF, the addition of GNS induced the β phase and disturbed the α crystals. The working mechanism of β-phase formation could have been that the GNSs provided the substrates of PVDF nucleation. The TTTT conformation chains (β-phase structure) were tethered on the surface of the GNS layers. These results indicate that the structure and properties of PVDF could be engineered upon the judicious

selection of crystallization conditions and the use of GNSs.

The authors thank the Analytical and Testing Center of Huazhong University of Science and Technology.

References

1. Lee, S. H.; Kim, M. W.; Kim, S. H.; Youn, J. R. Eur Polym J 2008, 44, 1620.
2. Amro, S.; Ratrick, L.; Yurii, G. Carbon 2010, 48, 3376.
3. Rama, K. L.; Sanjoy, S.; Dhruba, P. C.; Arun, K. N. Polymer 2010, 51, 5846.
4. Jiang, S. L.; Yu, Y.; Xie, J. J.; Wang, L. P.; Zeng, Y. K.; Fu, M.; Li, T. J Appl Polym Sci 2010, 116, 838.
5. Chen, S. T.; Yao, K.; Tay, F. E. H.; Chew, L. L. S. J Appl Polym Sci 2010, 116, 3331.
6. He, X. J.; Yao, K. Appl Phys Lett 2006, 89, 112909.
7. Lovinger, A. J. Science 1983, 220, 1115.
8. Marega, C.; Marigo, A. Eur Polym J 2003, 39, 1713.
9. Chen, S. T.; Yao, K.; Tay, F. E. H.; Chew, L. L. S. J Appl Polym Sci 2010, 116, 3331.
10. Hilczer, B.; Kulek, J.; Smogor, H. Ferroelectric 1999, 225, 33.
11. Ma, W. Z.; Zhang, J.; Chen, S. J.; Wang, X. L. J Macromol Sci Part B 2008, 47, 434.
12. Salimi, A.; Yousefi, A. A. J Polym Sci 2004, 42, 3487.
13. Park, Y. J.; Kang, Y. S.; Park, C. Eur Polym J 2005, 41, 1002.
14. Yuan, J. K.; Dang, Z. M.; Yao, S. H.; Zha, J. W.; Zhou, T.; Li, S. T.; Bai, J. B. J Mater Chem 2010, 20, 1441.
15. Elashmawi, I. S. Cryst Res Technol 2007, 42, 389.
16. Wang, Q. P.; Jiang, S. L.; Zhang, Y. Y.; Zhang, G. Z.; Xiong, L. Y. Polym Bull 2010, 66, 821.
17. Huang, X. Y.; Jiang, P. K.; Kim, C.; Liu, F.; Yin, Y. Eur Polym J 2009, 45, 377.
18. Lund, A.; Gustafsson, C.; Bertilsson, H.; Rychwalski, R. W. Compos Sci Technol 2011, 71, 222.
19. Bao, S. P.; Liang, G. D.; Tjong, S. C. Carbon 2011, 49, 1758.
20. Costa, P.; Silva, J.; Sencadas, V.; Costa, C. M.; Hattum, F. W. J. V.; Rocha, J. G.; Lanceros-Mendez, S. Carbon 2009, 47, 2590.
21. Gomes, J.; Nunes, J. S.; Sencadas, V.; Lanceros-Mensdez, S. Smart Mater Struct 2010, 19, 065010.
22. Sencadas, V.; Gregorio, R. J. R.; Lanceros-Mendez, S. J Macromol Sci Phys 2009, 48, 514.
23. Kim, Y. J.; Ahn, C. H.; Choi, M. O. Eur Polym J 2010, 46, 1957.
24. Peng, Q. Y.; Cong, P. H.; Liu, X. J.; Liu, T. X.; Huang, S.; Li, T. S. Wear 2009, 266, 713.
25. Ince-Gunduz, B. S.; Alpern, R.; Amare, D.; Crawford, J.; Dolan, B.; Jones, S.; Kobylarz, R.; Reveley, M.; Cebe, P. Polymer 2010, 51, 1485.
26. Shah, D.; Maiti, P.; Gunn, E.; Schmidt, D. F.; Jiang, D. D.; Batt, C. A.; Giannelis, E. P. Adv Mater 2004, 16, 1173.
27. Yu, L.; Cebe, P. Polymer 2009, 50, 2133.
28. Novoselov, K. S.; Geim, A. K.; Morozov, S. V.; Jiang, D.; Katsnelson, M. I.; Grigorieva, I. V.; Dubonos, S. V.; Firsov, A. A. Nature 2005, 438, 197.
29. Geim, A. K.; Novoselov, K. S. Nat Mater 2007, 6, 183.
30. Hernandez, Y.; Lotya, M.; Rickard, D.; Berbgin, S. D.; Coleman, J. N. Langmuir 2010, 26, 3208.
31. Tashiro, K.; Kobayashi, M.; Tadokoro, H. Macromolecules 1981, 14, 1757.
32. Bachmann, M. A.; Lando, J. B. Macromolecules 1981, 14, 40.
33. Nakagawa, K.; Ishida, Y. J Polym Sci Polym Phys Ed 1973, 11, 1503.
34. Jungnickel, B. J. In Polymeric Materials Handbook; Salamone, J. C., Ed.; CRC: New York, 1996; p 7115.
35. Vaia, R. A.; Giannelis, E. P. Macromolecules 1997, 30, 8000.